Structural connectivity reproducibility through multiple acquisitions

Authors:
Girard, G., Whittingstall, K., Deriche, R., Descoteaux, M.

Introduction:
Diffusion-weighted imaging is often used to reconstruct white matter (wm) pathways between brain areas for in vivo brain connectivity. In this study, we investigate the reproducibility and the specificity of connectivity matrices [Hagmann et al, 2007] in cortical to cortical connectivity using probabilistic and deterministic local streamline tractography, seeding both from the whole white matter and from wm-grey matter (gm) interface.

Methods:
Diffusion-weighted images were acquired on 3 volunteers (V1, V2, V3) along 64 uniformly distributed directions using a b-value of 1000 s/mm2, a single-shot echo-planar imaging sequence on a 1.5 Tesla SIEMENS Magnetom (128×128matrix, 2 mm isotropic resolution, TR/TE 11000/98 ms) and a GRAPPA factor of 2. An additional b0 image was acquired in reversed phase-encode direction to correct for susceptibility-induced distortions using FSL [Andersson et al., 2003]. An anatomical T1-weighted 1 mm isotropic MPRAGE (TR/TE 6.57/ 2.52 ms) image was also acquired. The whole sequence was repeated 4 times (A1, A2, A3, A4) for each volunteer.

The T1-weighted image was linearly registered to an upsampled b0 image using FSL/FLIRT [Jenkinson and Smith, 2001]. Freesurfer [Fischl et al., 2004] was then used to obtain the cortical parcellation from the registered T1-weighted image of 150 regions [Destrieux et al, 2009]. Each of the 150 gm regions were merged with their associated wm region to compute the connectivity between pairs of regions (number of streamlines connecting 2 regions) using Dipy (www.dipy.org) [Garyfallidis et al., 2014].

Fiber Orientation Distribution Functions from spherical deconvolution [Tournier et al., 2007] were used for tractography. Partial volume estimation maps from the T1-weighted image were obtained using FSL/Fast [Zhang et la., 2001] and used in the tracking process to enforce gm to gm connectivity [Girard et al., 2014]. Streamlines were generated seeding from both the wm mask using 5 seeds per voxel and the wm-gm interface using 10 seeds per voxel. This results in an average of 222,084 streamlines connecting regions of the cortex using wm seeding and 172,772 streamlines using wm-gm interface seeding. Every connectivity matrices C are normalized to sum to 1. The difference between 2 connectivity matrices is computed using $\sum|C1-C2|/2$. This can be interpreted as the fraction of streamlines connecting different regions in both matrices.

We used the Dunn index (DI) [Dunn, 1973] to evaluate both the intra-subject similarity of the connectivity matrices and the inter-subject differences. DI is computed as the average distance of intra-subject connectivity matrices over the average distance of inter-subject connectivity matrices.

Results:

Figure 1 shows example of connectivity matrices. Figure 2 shows the distances between each matrix of the 4 pipelines and Table 1 shows their associated DI.

Connectivity matrices (see Figure 1) from all pipelines show consistency for both inter- and intra-

subject distances (see Figure 2). Probabilistic tractography have a higher DI (1.63) than deterministic tractography (1.39). Interface seeding produces both a lower inter- and intra-subject distances than wm seeding. Furthermore, interface seeding is preferable to wm seeding since it limits the bias in the streamline distribution introduced by the over seeding in longer bundles [Girard et al., 2014, Hagmann et al., 2007]. Overall, the probabilistic wm-gm interface tractography has an average of 16.8% of streamlines connecting different brain regions for intra-subject reconstructions, 27.3% for inter-subject reconstructions.

Conclusions:

In this study, we showed that with the chosen acquisition scheme, probabilistic tractography pipelines produce connectivity matrices with the highest ratio of inter-subject distances to intra-subject distances. Moreover, we showed that connectivity matrices can be used as a tool to compare tractography algorithms in terms reproducibility and specificity.

References:

Andersson, J. L. R., Skare, S., & Ashburner, J. (2003). How to correct susceptibility distortions in spin-echo echo-planar images: application to diffusion tensor imaging. NeuroImage, 20(2), 870–88.

Destrieux, C., Fischl, B., Dale, A., & Halgren, E. (2010). Automatic parcellation of human cortical gyri and sulci using standard anatomical nomenclature. NeuroImage, 53(1), 1–15.

Dunn, J. C. (1973). A Fuzzy Relative of the ISODATA Process and Its Use in Detecting Compact Well-Separated Clusters. Journal of Cybernetics,3 (3), 32–57.

Fischl, B. (2004). Automatically Parcellating the Human Cerebral Cortex. Cerebral Cortex, 14(1), 11–22.

Garyfallidis, E., Brett, M., Amirbekian, B., Rokem, A., Van Der Walt, S., Descoteaux, M., & Nimmo-Smith, I. (2014). Dipy, a library for the analysis of diffusion MRI data. Frontiers in Neuroinformatics, 8.

Girard, G., Whittingstall, K., Deriche, R., & Descoteaux, M. (2014). Towards quantitative connectivity analysis: reducing tractography biases. NeuroImage, 98, 266–278.

Hagmann, P., Kurant, M., Gigandet, X., Thiran, P., Wedeen, V. J., Meuli, R., Thiran, J.-P., Jan. (2007). Mapping human whole-brain structural networks with diffusion MRI. PloS one 2 (7).

Jenkinson, M., & Smith, S. (2001). A global optimisation method for robust affine registration of brain images. Medical Image Analysis, 5(2), 143–156.

Tournier, J.-D., Calamante, F., & Connelly, A. (2007). Robust determination of the fibre orientation distribution in diffusion MRI: non-negativity constrained super-resolved spherical deconvolution. NeuroImage, 35(4), 1459–1472.

Zhang, Y., Brady, M., & Smith, S. (2001). Segmentation of brain MR images through a hidden Markov random field model and the expectation-maximization algorithm. IEEE Transactions on Medical Imaging, 20(1), 45–57. doi:10.1109/42.906424

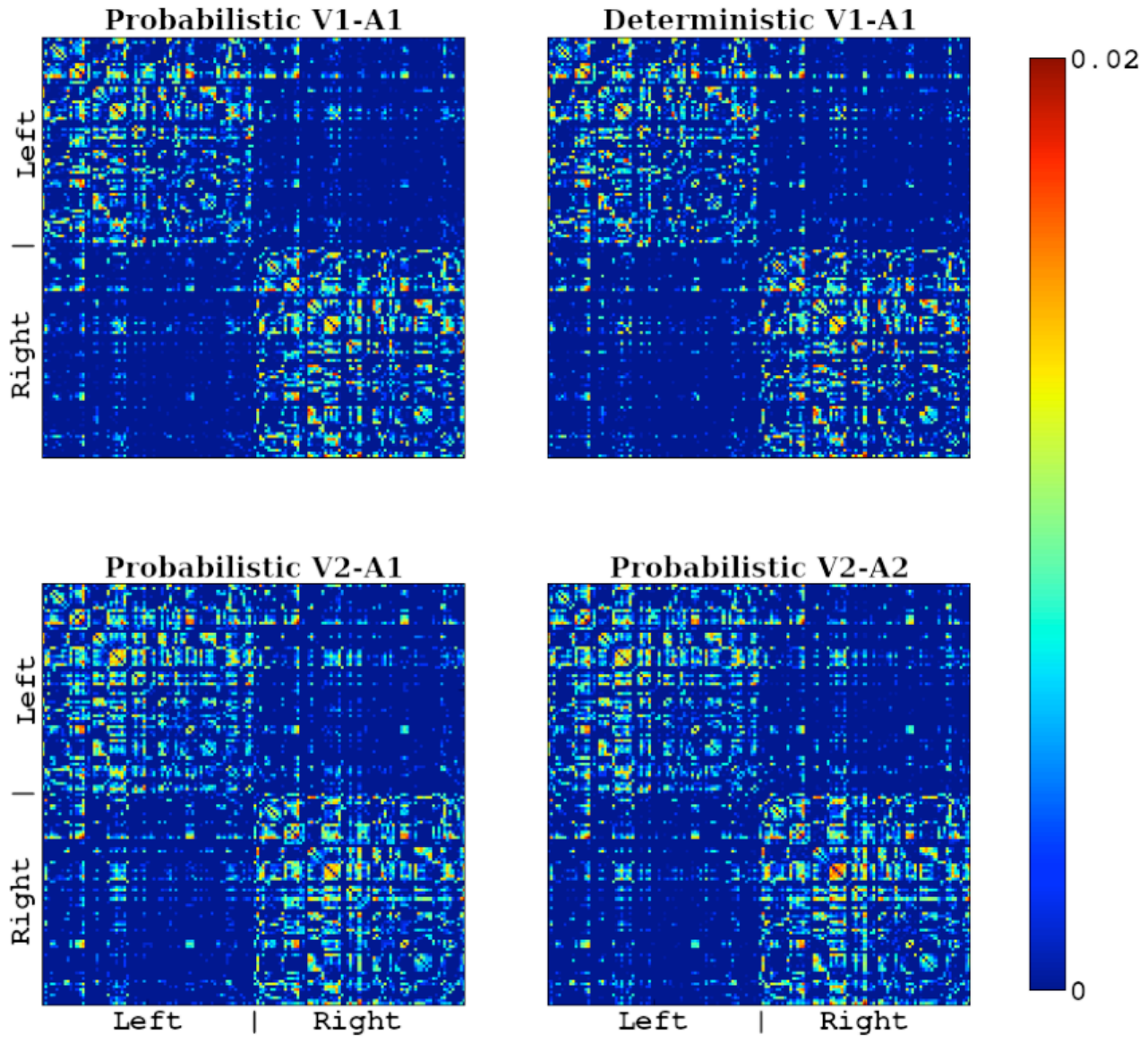

Figure 1: Connectivity matrices using wm-gm interface seeding. The first row shows connectivity matrices of deterministic and probabilistic tractography for the same subject and acquisition. The second row shows the connectivity matrices of probabilistic tractography for two acquisition of the same subject.

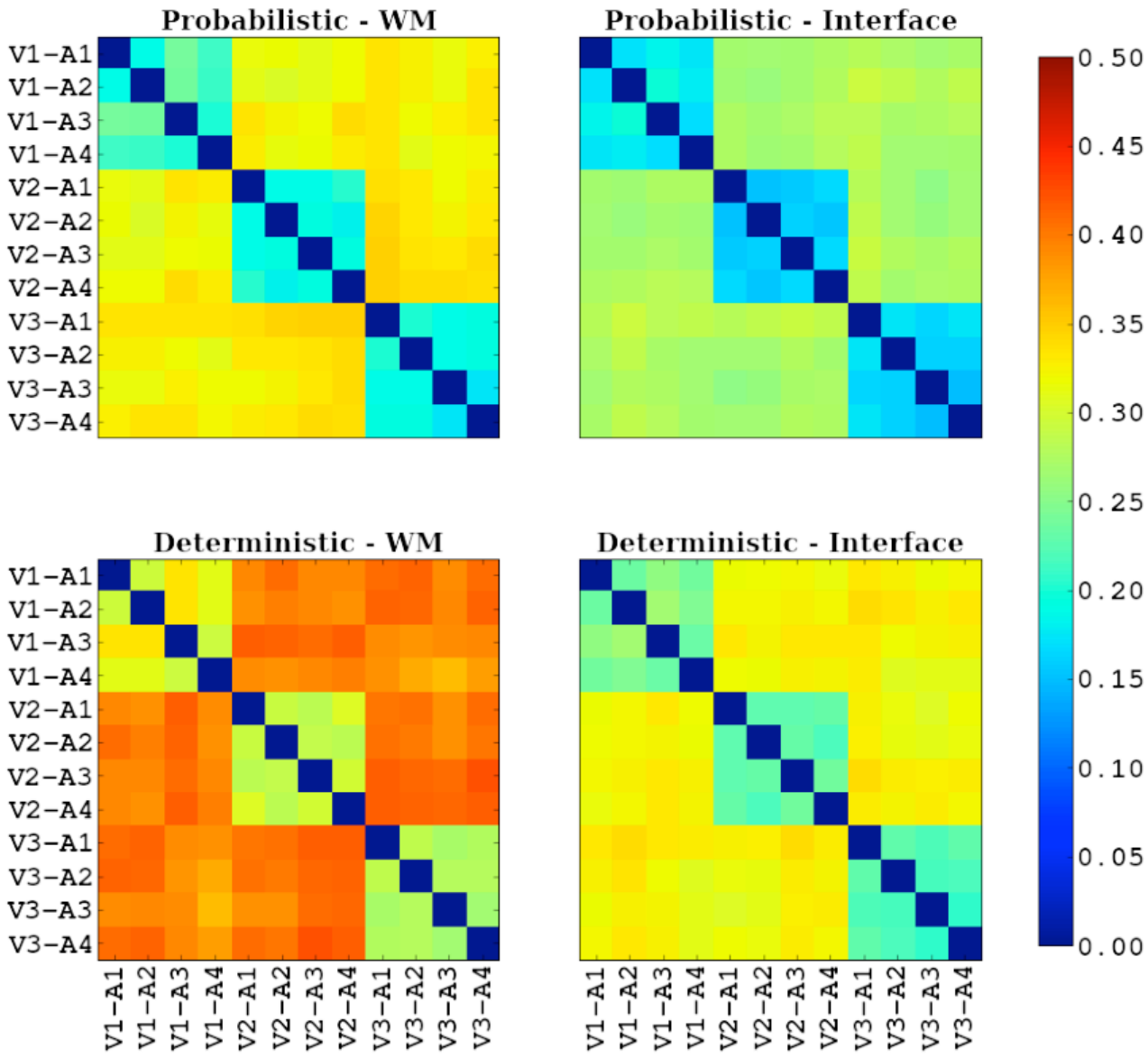

Figure 2: Distance between connectivity matrices. The distance between two connectivity matrices C_i is computed as $\sum |C_1 - C_2|/2$. The first row shows the probabilistic tractography pipelines and the second row the deterministic tractography pipelines. Distance ranges vary among pipelines, but consistently shows lower values for inter-subject than inter-subject connectivity matrices.

	Tractography			
	Deterministic		Probabilistic	
	WM	Interface	WM	Interface
Inter-subject distance	39.9%	32.3%	32.7%	27.3%
Intra-subject distance	29.4%	23.2%	19.9%	16.8%
Dunn index	1.36	1.39	**1.64**	**1.63**

Table 1: Connectivity matrix analysis. The distance between two connectivity matrices C_i is computed as $\sum |C_1 - C_2|/2$. The inter-subject distance is computed has the average distance between pairs of matrices of different brains. The intra-subject distance is computed has the average distance between pairs of matrices of the same brain. The Dunn index (DI) is the ratio of inter- to intra-subject distances. Probabilistic tractography shows a higher DI than deterministic tractography. WM-GM interface seeding reduces both the intra-subject and inter-subject distance compared to WM seeding strategy.